

RADIOSYNTHESIS OF 4'-(METHYL-¹¹C)THIOTHYMIDINE FOR IMAGING OF DNA SYNTHESIS *IN VIVO*

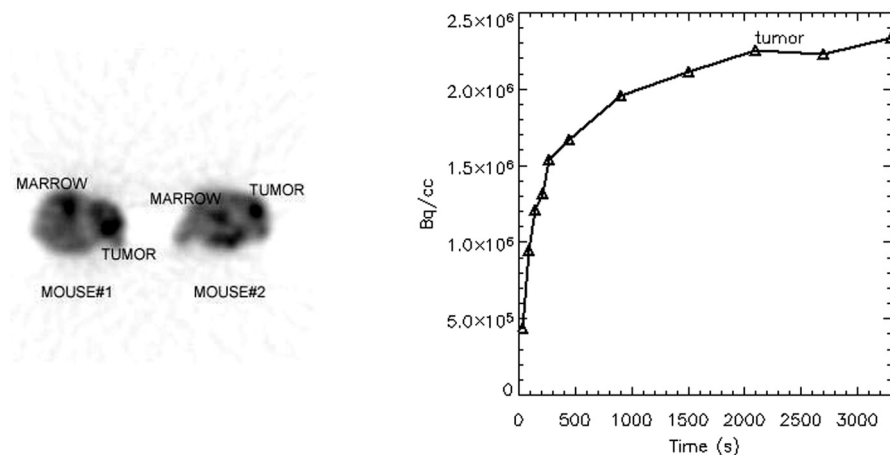
J. TOYOHARA, M. OKADA, C. TORAMATSU, T. FUKUMURA, K. TAKAHASHI, K. FUKUSHI, K. SUZUKI and T. IRIE

Molecular Imaging Center, National Institute of Radiological Sciences, Chiba, Japan

Introduction: We recently evaluated that 4'-[methyl-¹⁴C]thiothymidine ([methyl-¹⁴C]S-dThd) is a novel thymidine analog for simplified ¹¹C-PET imaging of DNA synthesis in cell proliferation (Toyohara et al., *J Nucl Med* 2006; **47**:1717-1722). Our results suggest that [methyl-¹⁴C]S-dThd closely resembles the biochemistry in anabolic metabolism and might be used as an alternative to [2-¹¹C]thymidine. Here, we carried out ¹¹C-labeling of 4'-thiothymidine and evaluated the feasibility of using the tracer to image cellular proliferation by PET.

Experimental: [Methyl-¹¹C]S-dThd was synthesized by rapid methylation of 5-trimethylstannyl-precursor *via* a palladium mediated Stille coupling reaction with ¹¹C-methyl iodide. Resultant [methyl-¹¹C]S-dThd was purified by the semi-preparative HPLC. The *in vivo* potential of [methyl-¹¹C]S-dThd was evaluated by studying its biodistribution in EMT-6 tumor-bearing mice. A dynamic scan was performed in mice with a microPET scanner.

Results and Discussion: A simple one-pot synthesis produced >20 mCi (740 MBq) of radiochemically pure [methyl-¹¹C]S-dThd, with a specific activity >15GBq/μmol at 30 min after end of bombardment (EOB) and 25% radiochemical yield (EOB); 7% end of synthesis (EOS). At 60 min after injection, [methyl-¹¹C]S-dThd uptake was highest in the proliferating tissues (mean SUVs: spleen, 6.2; tumor, 1.6; thymus, 1.1), whereas the non-proliferative tissues showed little uptake (mean SUVs: liver, 1.0; kidney, 0.6; lung, 0.4; muscle, 0.3; heart, 0.3). MicroPET imaging clearly demonstrated high uptake in the proliferating tissues such as tumor and marrow. The dynamic analysis showed accumulative uptake of the tracer in tumor over 60 min.



Conclusion: These results indicate that [methyl-¹¹C]S-dThd may be useful for measuring DNA synthesis with PET.

Acknowledgement: We also thank the crew of the Cyclotron Operation Section and Radiopharmaceutical Chemistry Section of National Institute of Radiological Sciences for their support in the operation of the cyclotron and production of radioisotopes.

Keywords: Thymidine, Proliferation, Radiosynthesis, Tumor, Positron Emission Tomography

IN VITRO AND INVO EVALUATION OF 2-AMINO-6-⁽¹⁸F) FLUORO-9-(4-HYDROXY-3-HYDROXY-METHYLBUTYL) PURINE (6-⁽¹⁸F)FPCV) AS A NEW PET PROBE FOR IMAGING HSV1-tk REPORTER GENE EXPRESSION

H.C. CAI^{1,2}, L. ZHANG¹, D.Z. YIN¹, J. WANG³ and Y.X. WANG¹

¹Research Center of Radiopharmaceuticals, Shanghai Institute of Applied Physics, Chinese Academy of Sciences, Shanghai, China; ²Graduate School, Chinese Academy of Sciences, Beijing, China; ³Zhejiang-California Nanoscience Institute, Hangzhou, Zhejiang, China

Introduction: Herpes simplex virus type 1 thymidine kinase (HSV1-tk) reporter gene together with proper PET probes are playing an important role in gene therapy, stem cell therapy and many other fields. Penciclovir derivatives have shown good potential as lead compound for developing new PET probes for in vivo imaging HSV1-tk expression.

Experimental: 2-amino-6-⁽¹⁸F)fluoro-9-(4-hydroxy-3-hydroxy-methylbutyl)purine (6-⁽¹⁸F)FPCV) was prepared via a one-step labeling procedure and evaluated for monitoring the expression of herpes simplex virus type 1 thymidine kinase (HSV1-tk) reporter gene in vitro and in vivo. For the in vitro experiments, C6 rat glioma cells transfected with HSV1-tk (C6-tk) and control C6 cells were incubated with 6-⁽¹⁸F)FPCV for various period of time (30-180 min), and the percentage of radioactivity uptake by cells was measured. For in vivo studies, nude mice bearing both C6 and C6-tk tumors were given 40 μCi of 6-⁽¹⁸F)FPCV, and the mice were scanned at different time point using microPET.

Results and Discussion: Results showed 5.6 to 18.9 times higher uptake of probe in C6-tk cells than that in C6 cells. MicroPET imaging results showed a fast (15 min) accumulation of this probe in C6-tk tumors with an average ratio of 1.5 of activity accumulated in C6-tk tumors to C6 tumors. Unfortunately, images also showed high bone uptake due to in vivo de-fluorination.

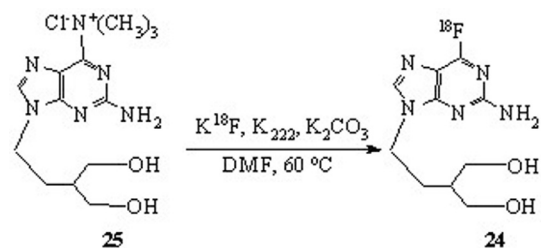


Fig. 1. Radiosynthesis scheme for 6-⁽¹⁸F)FPCV.

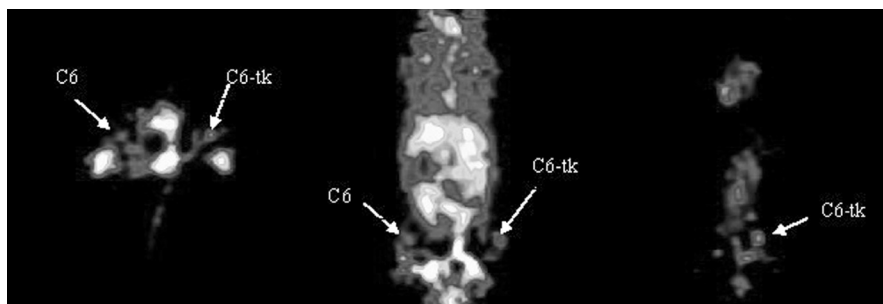


Figure 2. MicroPET images of nude mice bearing C6-tk and C6 tumors (10 min p.i.).

Conclusion: In conclusion, 6-⁽¹⁸F)FPCV showed its good potential as a PET probe for HSV-tk reporter gene expression in vitro and showed specific concentration in tumors with HSV-tk expression. Though the in vivo instability made the further application of the probe almost impossible, some of the results still encourage investigations for new HSV-tk probes in penciclovir derivatives.

Keywords: HSV1-tk, 6-FPCV, Reporter Gene, MicroPET, Fluorine-18

SYNTHESIS AND PRELIMINARY BIOLOGICAL EVALUATION OF AN IODINE-123 LABELED BI-CYCLIC NUCLEOSIDE ANALOG (BCNA) AS POTENTIAL SPECT REPORTER PROBE FOR VARICELLA-ZOSTER VIRUS THYMIDINE KINASE (VZV-tk) REPORTER GENE IMAGING

S.K. CHITNENI¹, C.M. DEROOSE², H. FONGE¹, R. GIJSBERS³, J. BALZARINI⁴, Z. DEBYSER³, L. MORTELMANS², A.M. VERBRUGGEN¹ and G.M. BORMANS¹

¹Laboratory for Radiopharmacy, University of Leuven; ²Division of Nuclear Medicine; ³Division of Molecular Medicine; ⁴Rega Institute for Medical Research, University of Leuven, Belgium

Introduction: BCNAs are highly potent and selective inhibitors of varicella-zoster virus (VZV). VZV-thymidine kinase (VZV-tk) efficiently phosphorylates these BCNAs to the corresponding 5'-monophosphates (MP) and the thymidylate kinase activity of VZV-tk further converts BCNA-5'-MP to BCNA-5'-diphosphates (Sienaert *et al.*, Mol. Pharmacol. 2002:249) that are trapped inside the cell. We recently synthesized and evaluated BCNA tracers labeled with F-18 or C-11 and this resulted in a new reporter gene/probe system. We report here the synthesis, biodistribution and cell uptake studies of an iodine-123 labeled BCNA.

Experimental: The phenol precursor 3-(2'-deoxy-*b*-D-ribofuranosyl)-6-(3-hydroxyphenyl)-2,3-dihydrofuro[2,3-*d*]pyrimidin-2-one (**1**) was synthesized as reported (McGuigan *et al.*, J. Med. Chem. 2000:4993) and converted to stable (**2**) as well as radioactive [¹²³I]-(**2**) mono-iodo derivative by electrophilic substitution using [^{127/123}I]-NaI. Affinity (IC₅₀) of (**1**) and (**2**) for VZV-tk was determined *in-vitro* in competition with [³H]-CH₃dThd. The biodistribution of (**3**) was evaluated in normal mice at 2 and 60 min p.i. Uptake of [¹²³I]-(**2**) was evaluated in 293T cells expressing VZV-tk or beta-galactosidase (control) that are incubated with [¹²³I]-(**2**) for 30 or 60 min.

Results and Discussion: The chemical yields of (**1**) and (**2**) were 38% and 47%, respectively. The RCY for [¹²³I]-(**2**) was 12 ± 1% (n=2) and RCP was >99%. The identity of [¹²³I]-(**2**) was confirmed by co-elution with the authentic non-radioactive compound (**2**) on RP-HPLC. LogP_{7.4} value of [¹²³I]-(**2**) was 0.83. The IC₅₀ values of (**1**) and (**2**) for VZV-tk were 2.6 and 4.2 μM, respectively. In mice, brain uptake of [¹²³I]-(**2**) was negligible at 2 min and 60 min after IV injection. Clearance from the blood was rapid (<3% ID at 60 min p.i.) and proceeded mainly by the hepatobiliary system (52.5% of ID at 60 min p.i.), and to a lesser extent by the urinary system (25.3% of ID at 60 min p.i.). The uptake of [¹²³I]-(**2**) in VZV-tk expressing cells was 1.74 and 1.4 fold higher at 30 and 60 min, respectively, compared to control cells (*P*<0.05).

Conclusion: A mono-iodo BCNA (**2**) was synthesized that has good affinity for the enzyme VZV-tk. On the basis of the specific retention of [¹²³I]-(**2**) in VZV-tk expressing cells *in-vitro*, further evaluation of this tracer as potential SPECT reporter probe in animal models is warranted.

Acknowledgement: This study was funded in part by the EC - FP6-project DiMI, LSHB-CT-2005-512146.

Keywords: BCNAs, VZV-tk, Gene Expression

PET IMAGING OF HERPES SIMPLEX ENCEPHALITIS IN RATS**J. DOORDUIN¹, E.F.J. DE VRIES¹, R.A. DIERCKX¹ and H.C. KLEIN^{1,2}**¹Nuclear Medicine and Molecular Imaging, University Medical Center Groningen, University of Groningen, Groningen, Netherlands; ²Center for Mental Health, Winschoten, Netherlands

Introduction: Approximately 80% of the human population is latently infected with the herpes simplex virus type-1 (HSV-1). HSV-1 is implicated in the etiology of neurological diseases like schizophrenia and Alzheimer's disease. In rodents, intranasal inoculation with HSV-1 results in mainly retrograde transneuronal transport of HSV-1 into the central nervous system (CNS), causing the activation of microglia. We used positron emission tomography (PET) to study active HSV-1 in the CNS (¹⁸F]FHBG) and the related microglia activation (¹¹C]PK11195) in a rat model of herpes simplex encephalitis (HSE). In addition, [¹⁸F]FDG was used to study the effect of herpes simplex encephalitis on CNS metabolism.

Experimental: Male Wistar rats were intranasally inoculated with HSV-1 (10⁷ PFU in 100µl PBS) or PBS (control). Within a week after the inoculation, replicating virus migrated into the CNS and induced microglia activation. At day 6 or 7 following inoculation the rats received an i.v. injection of [¹⁸F]FHBG (22±9 MBq), [¹¹C]PK11195 (78±22 MBq) or [¹⁸F]FDG (29±3 MBq). A dynamic PET scan (MicroPET Focus 220) was performed for 60 min, followed by ex vivo biodistribution.

Results and Discussion: At 60 min the uptake of [¹⁸F]FHBG (SUV) in HSE rats (n=8) was significantly higher (200-400%, p<0.05) in the bulbus olfactorius, anterior cingulate, frontal cortex and the parietal cortex as compared to controls (n=6). This is consistent with retrograde transneuronal transport of HSV-1 via olfactory epithelium into the CNS. However, there was a trend towards a higher uptake in all other areas. Microglia activation was found predominately in the brainstem and cerebellum, where the uptake of [¹¹C]PK11195 at 60 min was significantly higher (77% and 158%, p<0.05) in HSE rats (n=5) than in controls (n=5). Microglia activation in the brainstem, anterograde to the trigeminal nerve, could be the result of HSV-1 invading the trigeminal nerve, where it is known to establish latency. [¹⁸F]FDG showed a global increase in CNS metabolism, with a significantly higher (p<0.05) uptake (71.5±24.3%) in all brain areas of HSV-1 infected rats (n=8) as compared to control rats (n=4). It was an unexpected finding that focal HSV-1 infection caused distant microglia activation and global hypermetabolism.

Conclusion: The combination of [¹⁸F]FHBG, [¹¹C]PK11195 and [¹⁸F]FDG PET gave an unique insight in the special relationship between HSV-1 infection and specific foci of microglia activation with global hypermetabolism. This may provide a tool for better understanding of the role of HSV-1 infections in debilitating neurological diseases.

Acknowledgement: Stanley Medical Research Institute.

Keywords: HSV-1, Microglia, [¹⁸F]FHBG, [¹¹C]PK11195, MicroPET

DEVELOPMENT OF C-6 PYRIMIDINE DERIVATIVES AS THYMIDINE KINASE (TK) SUBSTRATES FOR GENE THERAPY MONITORING

M. MARTIC¹, A. JOHAYEM¹, M. HONER¹, L. SCAPOZZA², P.A. SCHUBIGER¹ and S.M. AMETAMEY¹

¹Center for Pharmaceutical Science of ETH, PSI and USZ, ETH Zurich, Zurich, Switzerland; ²Laboratoire de Chimie Thérapeutique, Section des Sciences Pharmaceutiques, Université de Genève, Geneva, Switzerland

Introduction: For human application of gene therapy, it is critically important to have a noninvasive imaging modality such as positron emission tomography (PET), which offers the possibility of monitoring the location, magnitude, and duration of gene expression over time. Our investigations were prompted by the need to develop PET imaging agents which lack the disadvantages of already existing reporter probes with herpes simplex virus type 1 thymidine kinase (HSV-1 TK), such as [¹⁸F]FHBG, which include cytotoxicity and unfavorable pharmacokinetics. Previous results with C-6 substituted pyrimidine derivative, [¹⁸F]fluoromethyl-HHT^[1], in tumor model using murine melanoma cell line B16 F1, showed that [¹⁸F]fluoromethyl-HHT is indeed far superior to [¹⁸F]FHBG due to greater sensitivity and contrast as well as lower levels of abdominal background radioactivity. However, it has the disadvantage of in vivo defluorination. Novel C-6 substituted pyrimidine derivatives are expected to be stable in vivo while retaining high sensitivity and ensuring image contrast.

Experimental: [¹⁸F]N-Methyl FHBT was prepared from an appropriate precursor using n.c.a. [¹⁸F]fluoride (K₂.2.2/K₂CO₃) in acetonitrile (30 min at 90°C). The protecting group was removed with 5% HCl in methanol (10 min at 90°C). Overall synthesis time was 80 minutes. Stability in aqueous medium of the reference compound N-Methyl FHBT and non-fluorinated derivative N-Methyl DHBT was assessed. For non-fluorinated derivative (N-Methyl DHBT), HPLC phosphorylation screening assay using HSV-1 TK, as well as, Km and Kcat experiments were performed.

Results and Discussion: Kinetic experiments showed that N-Methyl DHBT is phosphorylated at the similar rate to FHBG (Km=10±0.3μM; Kcat=0.036±0.015 sec⁻¹). Labeling of [¹⁸F]N-Methyl FHBT was achieved in 10-60% radiochemical yield (RCY) depending on reaction conditions. Maximum collected activity was 4.6 GBq. Two cartridge purifications ensured complete removal of free [¹⁸F]F⁻ and non-reacted precursor. Both N-Methyl DHBT and N-Methyl FHBT are stable in aqueous medium at room temperature over 6 months.

Conclusion: These preliminary data show that [¹⁸F]N-Methyl FHBT would be a good PET tracer for imaging HSV-1 TK expression in vivo.

References: [1] R. Blasberg, *European Journal of Cancer*, **38** (2002), 2137-2146. [2] S. Raic-Malic et al., *Nucleosides, Nucleotides & Nucleic Acids*, **23** (2004), 1707-1721.

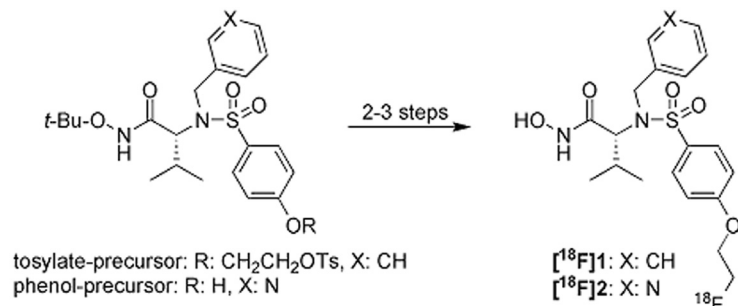
FLUORINATED DERIVATIVES OF THE POTENT MATRIX METALLOPROTEINASE INHIBITORS CGS 25966 AND CGS 27023A: (RADIO)SYNTHESES AND *IN VITRO* EVALUATION

S. WAGNER, H.J. BREYHOLZ, M.P. LAW, A. FAUST, C. HOELTKE, O. SCHOBER, M. SCHAEFERS and K. KOPKA

Department of Nuclear Medicine, University Hospital Muenster, Muenster, Germany

Introduction: Matrix metalloproteinases (MMPs) belong to a huge family of proteolytic enzymes. On the one hand, they participate in physiological tissue remodelling processes which require the disruption of extracellular matrix (ECM). On the other hand, elevated MMP expression and activity has been found in numerous diseases, including inflammation, cancer and atherosclerosis. The hydroxamic acids CGS 25966 and CGS 27023A represent potent broad-spectrum MMP inhibitors (MMPIs) and the radioiodinated derivative HO- ^{123}I -CGS 27023A was shown to specifically image activated MMPs in vascular lesions of apolipoprotein E-deficient mice *in vivo*. Our continuative studies focussed on the development of F-18-labelled CGS analogues, potentially useful as PET tracers.

Experimental: The fluorinated CGS 25966 (*N*-hydroxy-2(*R*)-[[[4-(2-fluoroethoxy)phenyl]-sulfonyl](benzyl)-amino]-3-methyl-butanamide) **1** and CGS 27023A (*N*-hydroxy-2(*R*)-[[[4-(2-fluoroethoxy)phenyl]-sulfonyl](3-picoly)-amino]-3-methyl-butanamide) **2** derivatives were synthesized and evaluated in MMP-2 and MMP-9 fluorogenic assays. The radiosyntheses of the radiofluorinated counterparts [^{18}F]**1** and [^{18}F]**2** were achieved in semi-automated 2-3 step sequences (Scheme 1).



Scheme 1

Results and Discussion: Target compounds **1** and **2** were achievable in 5-6 step syntheses with overall chemical yields of 5 and 31%, respectively. They possess high to moderate lipophilicities (clog D = 4.03 and 2.53, respectively) and maintain a high MMP binding potency against MMP-2 and MMP-9 (IC₅₀ = 2-50 nM) compared to the lead compounds CGS 25966 (K_i = 11-13 nM) and CGS 27023A (IC₅₀ = 11-60 nM). The radiosyntheses of [^{18}F]**1** was performed starting from a tosylate-precursor in two steps with a radiochemical yield of 12% (decay-corrected). Compound [^{18}F]**2** was prepared in 3 steps from the corresponding phenol-precursor with a radiochemical yield of 13% (decay-corrected) (Scheme 1).

Conclusion: The new compounds **1** and **2** shaped up as potent MMPIs *in vitro*. Suitable radiosyntheses for the labelled counterparts [^{18}F]**1** and [^{18}F]**2** were successfully developed for the subsequent *in vivo* evaluation using small-animal PET in combination with animal models characterized by dysregulated MMP-levels.

Acknowledgement: This study was supported by grants from the Deutsche Forschungsgemeinschaft (DFG), Sonderforschungsbereich 656 MoBil, Muenster, Germany (projects A2 and B1).

Keywords: Hydroxamic Acids, Matrix Metalloproteinases, MMP Inhibitors, CGS 25966, CGS 27023A

SYNTHESIS AND BIOLOGICAL EVALUATION OF INHIBITORS OF THE MITOCHONDRIAL COMPLEX 1 (MC-I) AS POTENTIAL POSITRON EMISSION TOMOGRAPHY (PET) CARDIAC IMAGING AGENTS

H.S. RADEKE, A. PUROHIT, K. HANSON, R. BENETTI, M. YU, M. MISTRY, M. GUARALDI, M. HAYES, P. YALAMANCHILI, M. KAGAN, J. LAZEWATSKY, D.S. EDWARDS, S. ROBINSON and D. CASEBIER

Research and Development, Bristol-Myers Squibb Medical Imaging, N. Billerica, MA, USA

Introduction: Coronary artery disease (CAD) is currently the leading cause of morbidity and mortality in developed nations. In order to evaluate regional myocardial blood flow and viability under rest or stress conditions, single-photon emission computed tomography (SPECT) based myocardial perfusion imaging agents (MPIA) such as ^{201}Tl or $^{99\text{m}}\text{Tc}$ complexes have become important tools in the management of CAD.

Recently, PET imaging has emerged as an alternate approach to evaluating myocardial blood flow. Prior in vitro and imaging studies with ^{125}I -iodorotenone (**2**, figure 1) demonstrated the superior extraction, retention and less "roll-off" of that agent versus $^{99\text{m}}\text{Tc}$ -sestamibi (CardioliteTM). Rotenone (**1**) is an insecticide that acts by early termination of the electron transport chain (ETC), which is embedded in the inner mitochondrial membrane. The natural product is a potent inhibitor of MC-I, the first enzyme complex in the ETC. The exceptional affinity of **2** for cardiac tissue is likely due to the very high weight percentage of mitochondria in cardiomyocytes, suggesting MC-I inhibition as an ideal target for the development of cardiac PET tracers.

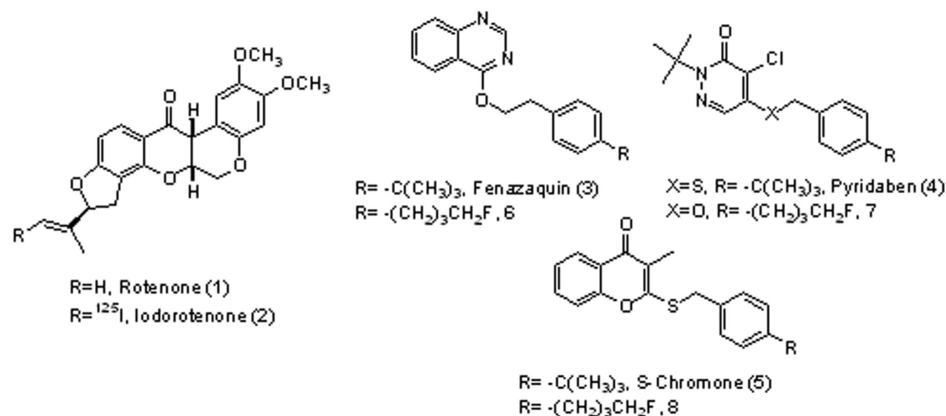


Fig. 1

Experimental: Additional classes of MC-I inhibitors have been reported such as fenazaquin (**3**), pyridaben (**4**), and S-chromone (**5**). Our goal was to incorporate PET radionuclide ^{18}F into analogs of **3-5** without adversely affecting the binding properties of the parent structure. A structure-activity relationship (SAR) study was carried out which identified the alkyl group on the phenyl ring to be the most tolerant and amenable site for chemical modification within these structures. Synthesis and biological evaluation of analogs in all three compound classes will be presented.

Results and Discussion: Binding studies identified analogs **6-8** as potent MC-I inhibitors (IC_{50} = 9-15 nM, Figure 2). Furthermore, bio-distribution (BioD) studies of [^{18}F]-**6**-[^{18}F]-**8** in SD rats demonstrated good heart uptake (1.80-3.13%ID/g, 60 minutes post injection), which complemented the results obtained in imaging studies in SD rats.

Conclusion: An overview of the SAR studies, BioD, and imaging data for **6-8** will be presented. These compounds represent a new generation of cardiac imaging agents.

Keywords: Mitochondrial Complex 1 Inhibitor, Positron Emission Tomography, Cardiac Imaging Agent